FLUORESCENT SCATTERING IN PLANETARY ATMOSPHERES
IV. FORMATION OF LYMAN-BIRGE-HOPFIELD BANDS OF N_2 IN THE TERRESTRIAL ATMOSPHERE

YOUSEF SOBOUTI
Yerkes Observatory, University of Chicago*
Received March 14, 1963

ABSTRACT

The intensities of the Lyman-Birge-Hopfield bands of N_2 produced by resonance and fluorescence mechanisms in the terrestrial upper atmosphere are calculated. Shortward of 1750 A, the band intensities are much stronger than the continuum resulting from Rayleigh scattering and may be amenable to measurement. In the near ultraviolet, however, they are completely overshadowed by the latter.

I. INTRODUCTION

Ultraviolet sunlight is expected to excite the atmospheric N_2 molecules and, thereby, cause the emission of the Lyman-Birge-Hopfield (LBH) bands of this molecule; the transitions in question are $a^1\Pi_g$–$X^1\Sigma_g^+$. The bands will then be diffusely reflected from the top of the atmosphere and form part of the daytime ultraviolet spectrum of the terrestrial atmosphere as observed from above.

Formation of the LBH bands in the atmosphere of Mars was investigated in Paper III (Sobouti 1963*b*) of this series. Along the same lines as for Mars, here we calculate the intensities of the LBH bands as reflected from the atmosphere of the earth. The main differences between the terrestrial and the Martian atmospheres are (*a*) in the terrestrial atmosphere the optical depth in the spectral lines is very small, and (*b*) the continuous absorption by O_2 is much stronger than in the atmosphere of Mars. Both these factors require a mathematical approach to the terrestrial problem different from the Martian one.

For details and many of the formulae needed in this paper we shall refer mainly to Paper III and also to Papers I and II of this series (Chamberlain and Sobouti 1962; Sobouti 1962). For comprehension of this paper, frequent reference to Paper III will be essential.

II. OPTICAL DEPTH OF THE ATMOSPHERE

The lower boundary of the scattering atmosphere is set at an altitude where the effect of collisions in depopulating the electronic state $a^1\Pi_g$ of the N_2 molecule becomes comparable with that of the radiative cascades from this state. From equation (18) of Paper III and from standard atmospheric models (e.g., see Chamberlain 1961, p. 576), one gets a density of 5×10^{13} particles per cm^3 at a temperature of about 150° K for this lower boundary of the scattering atmosphere. The altitude of the boundary is about 90 km, and there is a total number of 9×10^{19} N_2 molecules per cm^2 column above this height. According to atmospheric models, more than 90 per cent of these particles are confined to a thin slab from 90 to 115 km. We shall assume an O_2 concentration of 20 per cent (which gives a total number of 2.5×10^{18} O_2 molecules per cm^2 column) and a mean temperature of 155° K for this scattering slab.

These data, together with the line absorption coefficient of N_2 and the absorption cross-section of O_2, suffice to calculate the optical depth of the atmosphere both in the spectral lines and in the continuum. Table 1 gives the optical depth at the center of

* Present address: Department of Mathematics, King's College, Newcastle upon Tyne, England.

the resonant P, Q, R lines, $\tau_i(v'J', v'' = 0)$ (where $i = P, Q, R$), of the LBH system. These values are calculated from equations (20) and (1) of Paper III. Table 2 gives the optical depth in the continuum, $\tau_\sigma(v', v'')$, at frequencies of the LBH bands. They are calculated from equation (20) of Paper III.

III. INTENSITIES OF RESONANT BANDS

The resonant bands ($v'' = 0$) with $v' = 0$, 1, 2, 3, 4, 7, and 9 have larger optical depths in their continuum (see Table 2). The total optical depth of a rotational line in these bands, $\tau_i(v'J', v'' = 0) + \tau_\sigma(v', v'' = 0)$, will also be large. For these transitions the atmosphere may be regarded as an optically infinite one. The resonant bands with $v' = 5$, 6, and 8, on the other hand, have considerably smaller depth in the continuum. They are affected very little by O_2 absorption and contribute the most to the scattered intensities. We shall treat these transitions with the theory of finite atmospheres.

a) Transitions Originating from $v' = 0, 1, 2, 3, 4, 7,$ and 9 Levels

Formation of a resonant band in an optically semi-infinite atmosphere and with the O_2 absorption is discussed in Section VI of Paper III. We quote only the final expression for the scattered integrated intensity of a resonant line given by equation (33) of that paper:

$$\mathfrak{I}_i(\mu) = \pi^{1/2} \frac{U\nu_c}{c} \frac{\mu_0}{4} \varpi_i \mathfrak{H}_i^{(c)}(\mu) \sum_j F_j \frac{k_j^{(c)} \mathfrak{H}_j^{(c)}(\mu_0)}{K_j^{(c)}\mu + K_i^{(c)}\mu_0}, \qquad (1)$$

$$i, j = P, Q, R .$$

b) Transitions Originating from $v' = 5,$ 6, and 8 Levels

In an optically finite atmosphere, the scattered monochromatic intensity in a direction μ is given by equations (9) and (74) of Paper II:

$$I_i(\mu) = \frac{\mu_0}{4} \varpi_i \sum_j F_j \frac{k_j [\mathfrak{X}_i(\mu)\mathfrak{X}_j(\mu_0) - \mathfrak{Y}_i(\mu)\mathfrak{Y}_j(\mu_0)]}{K_j\mu + K_i\mu_0}, \qquad (2)$$

where the $\mathfrak{X}$- and $\mathfrak{Y}$-functions are defined by equations (78) and (79) of Paper II. The rest of the notation is explained in Paper III. As in equations (27) and (32) of Paper III, we integrate equation (2) over the profile of the spectral line, obtaining

$$\mathfrak{I}_i(\mu) = \frac{U\nu_c}{c} \frac{\mu_0}{4} \varpi_i \sum_j F_j [\mathfrak{X}_i^{(c)}(\mu)\mathfrak{X}_j^{(c)}(\mu_0) - \mathfrak{Y}_i^{(c)}(\mu)\mathfrak{Y}_j^{(c)}(\mu_0)] \times \int \frac{k_j}{K_j\mu + K_i\mu_0} dx, \qquad (3)$$

$$i, j = P, Q, R$$

In writing this equation we have made use of the fact that the $\mathfrak{X}$- and $\mathfrak{Y}$-functions are slowly varying functions of frequency through the dependence of the absorption coefficients k_i's and K_i's on the frequency (see eqs. [1] and [31] of Paper III). A superscript (c) in equation (3) indicates that the quantity in question is to be evaluated at the center of the line profile. The integral in equation (3) is evaluated by Laplace's method (see n. 3 of Paper III) if continuous absorption predominates over the line absorption. Otherwise it is evaluated numerically within its limits $\pm \ln^{1/2}2$. These limits correspond to those frequencies at which the line optical depth drops to half its value at the center of the line profile (see the expression for the line optical depth preceding eq. [30] of Paper III). Equations (42) and (43) of Paper II provide two approximate

TABLE 1

OPTICAL DEPTH AT THE CENTER OF THE RESONANCE LINES OF THE LBH BANDS

v' \ J'	1	2	3	4	5	6	7	8	9	10	11	12	13	14	15
							$\tau_P(v'J', v''=0)$								
0	.11	.19	.24	.27	.27	.25	.21	.18	.14	.10	.07	.05	.03	.02	.01
1	.28	.51	.66	.72	.72	.67	.58	.47	.37	.27	.19	.13	.08	.05	.03
2	.42	.75	.97	1.07	1.07	.99	.85	.70	.54	.40	.28	.19	.12	.07	.04
3	.45	.80	1.03	1.14	1.14	1.06	.91	.75	.58	.42	.30	.20	.13	.08	.05
4	.39	.70	.90	1.00	1.00	.92	.80	.65	.50	.37	.26	.17	.11	.07	.04
5	.30	.53	.68	.76	.76	.70	.60	.49	.39	.28	.20	.13	.08	.05	.03
6	.20	.36	.47	.52	.52	.48	.41	.34	.26	.19	.13	.09	.06	.04	.02
7	.13	.23	.29	.33	.33	.30	.26	.21	.16	.12	.09	.06	.04	.02	.01
8	.08	.14	.18	.19	.19	.18	.15	.13	.10	.07	.05	.03	.02	.01	.01
9	.04	.08	.10	.11	.11	.10	.09	.07	.06	.04	.03	.02	.01	.01	
							$\tau_Q(v'J', v''=0)$								
0	.34	.53	.66	.73	.74	.70	.62	.52	.42	.32	.23	.16	.11	.07	.04
1	.92	1.42	1.72	1.97	1.99	1.88	1.67	1.40	1.12	.85	.62	.43	.29	.18	.11
2	1.35	2.09	2.62	2.90	2.94	2.77	2.46	2.07	1.65	1.26	.91	.63	.42	.27	.16
3	1.45	2.24	2.80	3.10	3.15	2.97	2.64	2.22	1.77	1.35	.98	.68	.45	.29	.17
4	1.27	1.96	2.45	2.71	2.75	2.60	2.31	1.94	1.55	1.18	.85	.59	.39	.25	.15
5	.96	1.48	1.85	2.05	2.08	1.97	1.75	1.47	1.17	.89	.65	.45	.30	.19	.12
6	.65	1.01	1.27	1.40	1.42	1.34	1.19	1.00	.80	.61	.44	.31	.20	.13	.08
7	.41	.64	.80	.88	.90	.85	.75	.63	.50	.38	.28	.19	.13	.08	.05
8	.25	.38	.48	.53	.53	.50	.45	.38	.3.	.20	.17	.11	.08	.05	.03
9	.14	.21	.27	.30	.30	.28	.25	.21	.17	.13	.09	.07	.04	.03	.02
							$\tau_R(v'J', v''=0)$								
0	.24	.34	.42	.47	.49	.47	.43	.37	.31	.24	.18	.13	.09	.06	.04
1	.63	.92	1.13	1.27	1.31	1.27	1.16	1.00	.83	.65	.49	.35	.24	.16	.10
2	.94	1.35	1.67	1.87	1.93	1.87	1.71	1.48	1.22	.96	.72	.52	.35	.23	.15
3	1.00	1.45	1.79	2.00	2.07	2.00	1.83	1.58	1.30	1.02	.77	.55	.38	.25	.16
4	.88	1.27	1.57	1.75	1.81	1.75	1.60	1.38	1.14	.90	.67	.48	.33	.22	.14
5	.66	.96	1.19	1.32	1.37	1.32	1.21	1.05	.86	.68	.51	.37	.25	.17	.10
6	.45	.65	.81	.90	.93	.90	.83	.71	.59	.46	.35	.25	.17	.11	.07
7	.29	.41	.51	.57	.59	.57	.52	.45	.37	.29	.22	.16	.11	.07	.05
8	.17	.25	.30	.34	.35	.34	.31	.27	.22	.17	.13	.09	.06	.04	.03
9	.10	.14	.17	.19	.20	.19	.18	.15	.13	.10	.07	.05	.04	.02	.02

TABLE 2

CONTINUOUS OPTICAL DEPTH AT THE FREQUENCIES OF THE LBH BANDS, $\tau_\sigma(v', v'')$

v' \ v''	0	1	2	3	4	5	6	7	8	9	10	11	12	13
0	35.7	28.0	19.0	9.9	3.6	1.0	0.1							
1	36.2	33.0	25.7	16.2	7.5	2.8	0.2	0.1						
2	33.0	36.5	31.5	23.2	14.4	6.0	2.0	0.2						
3	17.7	33.7	36.2	29.2	20.3	11.7	4.6	1.5	0.2					
4	5.1	26.2	36.5	33.7	26.7	18.2	9.6	3.5	1.0					
5	1.3	5.6	32.5	36.5	32.5	24.6	15.6	7.2	2.2	0.5	0.1			
6	0.2	1.8	17.7	34.2	36.5	29.7	21.5	12.7	5.6	1.8	0.2			
7	3.7	1.2	5.2	24.5	36.2	36.0	27.2	19.0	10.4	4.1	1.3	0.2		
8	0.8	1.1	1.2	5.6	32.5	36.5	32.5	24.7	16.2	8.2	3.0	0.9		
9	47.5	0.5	0.3	5.1	17.7	34.2	36.5	29.5	21.7	13.9	6.2	2.2	0.3	0.1

expressions for the $\mathfrak{X}$- and $\mathfrak{Y}$-functions in terms of Chandrasekhar's X-, Y-, and related functions. These expressions, together with tables of the latter functions (Sobouti 1963*a*), have been used to calculate the necessary values of the $\mathfrak{X}$- and $\mathfrak{Y}$-functions in equation (3).

The total scattered intensity in a band is obtained by summing all the lines constituting that band. Hence

$$\mathfrak{I}(\mu) = \sum_{J'} \sum_{P,\,Q,\,R} \mathfrak{I}_i(\mu), \tag{4}$$

where $\mathfrak{I}_i(\mu)$ is given by either equation (1) or equation (3), depending on the optical depth of the atmosphere at the band in question.

IV. INTENSITIES OF FLUORESCENT BANDS

Equation (36) of Paper III gives the monochromatic intensity of a fluorescent line in terms of that of a corresponding resonant band:

$$I_i(\mu,\, v'') = \frac{\varpi_i(v'')}{\varpi_i(0)} \frac{K_i}{s_i(v'')} I_i\left(\frac{K_i\mu}{s_i(v'')},\ v'' = 0\right). \tag{5}$$

For a semi-infinite atmosphere, applicable to the lines with $v' = 0$, 1, 2, 3, 4, 7, and 9, equation (5) is reduced and integrated over the line profile in Paper III. The final result from equation (42) of that paper is

$$\mathfrak{I}_i(\mu,\, v'') = \pi^{1/2} \frac{U\nu_c}{c} \frac{\mu_0}{4} \varpi_i(v'')\, \mathfrak{H}_i^{(c)}\left(\frac{K_i\mu}{s_i(v'')}\right) \sum_j F_j \frac{k_j^{(c)} \mathfrak{H}_j^{(c)}(\mu_0)}{K_j^{(c)}\mu + s_i(v'')\mu_0}. \tag{6}$$

For finite atmospheres, which pertain to the transitions with $v' = 5$, 6, and 8, the resonant intensity on the right side of equation (5) is given by equation (2). Upon substitution for this quantity and integration over the line profile, one finds

$$\mathfrak{I}_i(\mu,\, v'') = \frac{U\nu_c}{c} \frac{\mu_0}{4} \varpi_i(v'')$$

$$\times \sum_j F_j \left\{ \mathfrak{X}_i^{(c)}\left[\frac{K_i\mu}{s(v'')}\right] \mathfrak{X}_j^{(c)}(\mu_0) - \mathfrak{Y}_i^{(c)}\left[\frac{K_i\mu}{s(v'')}\right] \mathfrak{Y}_j^{(c)}(\mu_0) \right\} \tag{7}$$

$$\times \int \frac{k_j}{K_j\mu + s(v'')\mu_0}\, dx.$$

The integral in this equation is treated in the same way as the one in equation (3).

The total intensity of a band is again given by summing all the lines as in equation (4).

V. RAYLEIGH SCATTERING

A general discussion of Rayleigh scattering, which is expected to produce the continuum of the reflected spectrum, is given in Section VIII of Paper III. Shortward of 1759 A, the onset of the Schumann-Runge continuum, O_2 strongly absorbs the sunlight. This, on the one hand, greatly reduces the effective albedo of the scattering (see eq. [43] of Paper III) and, on the other hand, increases the total optical depth of the atmosphere. Nevertheless, the optical depth corresponding to Rayleigh scattering remains very small. The scattering atmosphere may then be approximated by an optically semi-infinite one in which only the primary scattering is of importance. The intensity due to Rayleigh scattering is then given by (Chandrasekhar 1950, p. 146)

$$I_{\mathrm{Ray}}(\mu) = \tfrac{1}{4}\varpi F_\lambda \frac{\mu_0}{\mu + \mu_0}, \tag{8}$$

where ϖ is the albedo expressed by equation (43) of Paper III and πF_λ is the incident solar flux. In calculating the above intensity, the flux values were taken from Friedman (1961) and Hinteregger (1961).

Longward of 1759 A, O_2 absorption is very weak. Rayleigh scattering may extend down in the atmosphere as low as the ozone layer. The latter substance has extremely large absorption cross-sections compared with those for Rayleigh scattering (consult

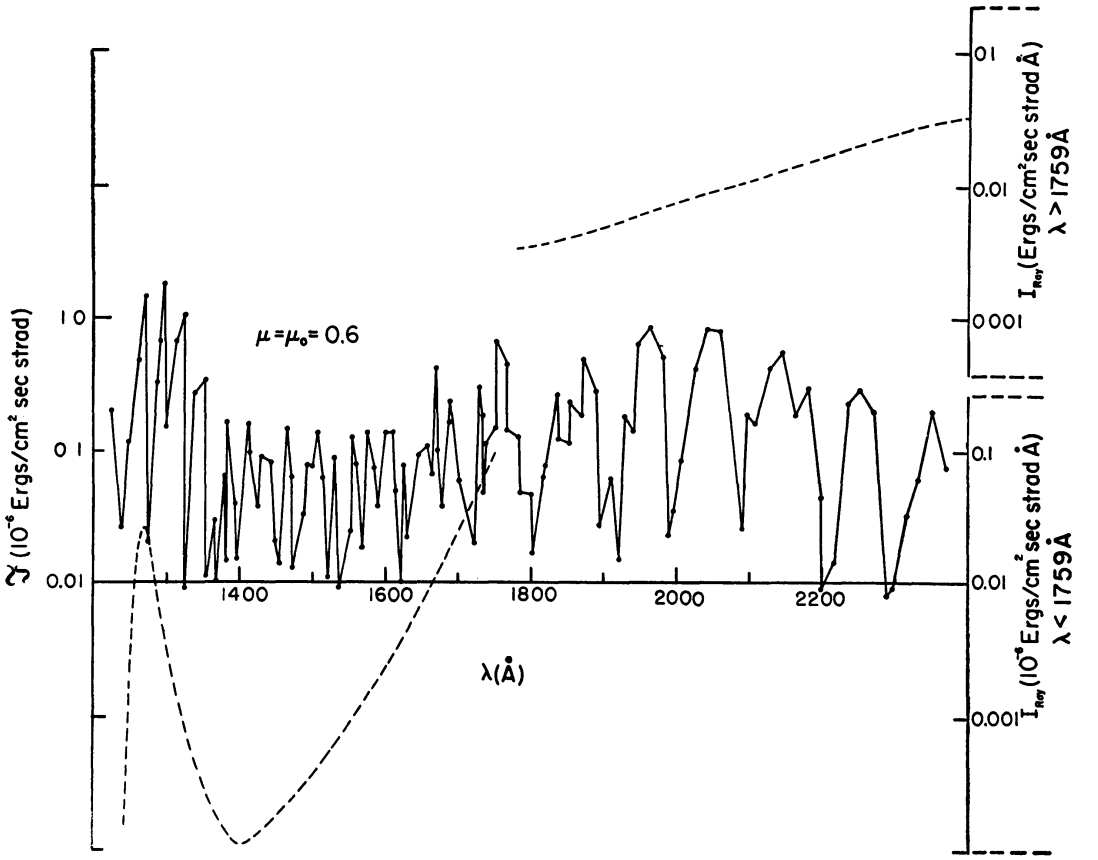

FIG. 1.—Diffusely reflected intensities of the LBH bands (both resonant and fluorescent) plotted versus wavelength. The dots are calculated intensities for entire bands and are taken from Table 4. The connecting lines have been drawn in only to increase the legibility of the plots. Estimates of the specific intensities of the bands may be obtained by dividing these total intensities by the widths of the corresponding resonant bands listed in Table 3. The dotted curve is the specific intensity of the continuum due to Rayleigh scattering. Note the two different scales for this continuum shortward and longward of 1759 A.

Table 3 of Paper III), so that the contribution to Rayleigh scattering from regions below the ozone layer may be neglected. The scattering atmosphere, i.e., that part of the atmosphere bounded on its lower edge by the ozone layer, will have a finite optical depth, and the Rayleigh intensity will be given by (Chandrasekhar 1950, pp. 161 and 181)

$$I_{\text{Ray}}(\mu) = \tfrac{1}{4}\varpi F_\lambda \frac{\mu_0}{\mu+\mu_0}[X(\mu)X(\mu_0) - Y(\mu)Y(\mu_0)], \tag{9}$$

where $X(\mu)$ and $Y(\mu)$ are Chandrasekhar's X- and Y-functions evaluated for the total optical depth of the scattering atmosphere, including both Rayleigh scattering and the O_2 absorption. The albedo ϖ is again given by equation (43) of Paper III. In both

equations (8) and (9) the approximation is made that the Rayleigh scattering takes place isotropically. From these equations the continuum intensity has been calculated and has been plotted in Figure 1. A discussion of these results is given in the following section.

VI. RESULTS AND DISCUSSION

The values of solar flux used to calculate the intensities of the LBH bands are given in Table 3. They are from Friedman (1961) and Hinteregger (1961). The table also includes the wavelengths of the resonant bands and the values of an effective width that is defined as the wavelength interval between the band head and that rotational line in the P-branch which contributes about 1 per cent to the intensity of the entire band. The specific intensity (i.e., the intensity per unit wavelength interval) may then be obtained by dividing the integrated intensity of the band by its effective width. The bands originating from $v' = 5$, 6, and 8, which are less affected by the O_2 absorption, have somewhat smaller widths than the others. This is because of the bracketed factor in equation (3), which falls off rapidly with the decreasing line optical depth corresponding to the higher rotational quantum numbers.

TABLE 3

ADOPTED SOLAR FLUXES INCIDENT ON THE UPPER ATMOSPHERE

(10^{-3} ergs/cm^2 sec A)

	v'									
	0	1	2	3	4	5	6	7	8	9
λ (A)	1450	1416	1384	1354	1325	1298	1273	1249	1227	1205
πF_λ	10	6	4	4	5	5	3	3	4	8
$\delta\lambda$ (A)	2 3	2 2	2 2	2 1	2 0	1 1	1 4	1 9	1 2	1 8

The calculated band intensities are listed in Table 4. As pointed out in Paper III, uncertainties in the values of the solar flux and therefore in the absolute band intensities which are directly proportional to the former are considerable. Nevertheless, the relative intensities of the bands arising from one and the same upper vibrational level, v', remain unaffected by errors in the flux values.

Generally speaking, the terrestrial spectrum constructed in this paper should be more accurate than the Martian spectrum constructed in Paper III. Thanks to our detailed knowledge of the earth's atmosphere, a realistic model based on direct observations has been employed in the calculation of the terrestrial spectrum. The situation was quite different insofar as the calculations carried out for the Martian atmosphere were concerned. In this latter, it was necessary to rely largely on theoretical inferences for the necessary information concerning the structure and composition of the atmosphere. Also, particular care has been taken to use more accurate mathematical techniques in calculating the band intensities and to employ more precise estimates for the effective widths of the lines and bands. Had these refinements been made in Paper III, the uncertainties in the input parameters for the Martian model would have obscured them and would have made their introduction meaningless.

In Figure 1 the band intensities are plotted as a function of the wavelength. The dip in the region 1300–1700 A produced by strong O_2 absorption is especially noteworthy. Such a dip does not exist in the upper diagram of Figure 3 in Paper III, which corresponds to a pure nitrogen atmosphere, or exists to a much lesser extent in the

1963ApJ...138..748S

INTENSITIES OF THE LBH BANDS (10^{-6} ERGS/CM2 SEC STRAD)
RESONANT BANDS $v''=0$, $\mu=0.0$

Table 4

μ_0	v' 0	1	2	3	4	5	6	7	8	9
0.20	0.041	0.186	0.308	0.670	2.022	3.562	3.405	0.236	0.412	0.007
0.40	0.041	0.186	0.309	0.671	2.032	3.591	3.434	0.236	0.413	0.007
0.60	0.041	0.186	0.309	0.672	2.038	3.608	3.450	0.236	0.413	0.007
0.80	0.041	0.186	0.309	0.672	2.042	3.620	3.460	0.236	0.413	0.007
1.00	0.041	0.186	0.309	0.673	2.045	3.628	3.466	0.237	0.413	0.007

INTENSITIES OF THE LBH BANDS (10^{8} ERGS/CM2 SEC STRAD)

Table 4

v''	0	1	2	3	4	5	6	7	8	9	10	11	12	13	14	15	16	17	18	19	20	21
v'	μ_0=0.20 μ=0.20																					
0	0.021	0.074	0.126	0.137	0.098	0.048	0.017	0.005	0.001													
1	0.093	0.148	0.062	0.	0.077	0.163	0.147	0.077	0.028	0.008	0.002											
2	0.154	0.077	0.003	0.086	0.073	0.	0.059	0.141	0.125	0.065	0.023	0.006										
3	0.336	0.015	0.080	0.076	0.004	0.132	0.106	0.	0.125	0.234	0.183	0.084	0.026	0.006								
4	1.017	0.010	0.154	0.	0.131	0.077	0.048	0.400	0.179	0.047	0.498	0.645	0.414	0.165	0.045	0.009						
5	1.735	0.282	0.062	0.037	0.063	0.011	0.135	0.022	0.230	0.641	0.064	0.286	0.871	0.826	0.425	0.140	0.032					
6	1.522	0.624	0.005	0.039	0.001	0.032	0.009	0.036	0.089	0.007	0.528	0.356	0.010	0.510	0.815	0.562	0.229	0.061	0.011			
7	0.118	0.320	0.009	0.029	0.006	0.014	0.004	0.024	0.001	0.065	0.020	0.047	0.114	0.015	0.035	0.129	0.127	0.065	0.021	0.004		
8	0.200	0.481	0.153	0.027	0.015	0.001	0.013	0.001	0.018	0.010	0.038	0.114	0.	0.223	0.135	0.005	0.193	0.299	0.201	0.077	0.019	
9	0.004	0.026	0.020	0.	0.011	0.001	0.005	0.002	0.005	0.002	0.007	0.000	0.008	0.001	0.004	0.007	0.001	0.003	0.009	0.008	0.004	0.001
	μ_0=0.20 μ=0.40																					
0	0.014	0.047	0.076	0.076	0.052	0.024	0.008	0.002	0.000													
1	0.062	0.097	0.039	0.	0.042	0.084	0.074	0.039	0.014	0.004	0.001											
2	0.103	0.052	0.002	0.054	0.043	0.	0.030	0.071	0.062	0.032	0.011	0.003										
3	0.224	0.011	0.059	0.054	0.003	0.081	0.059	0.	0.063	0.117	0.091	0.042	0.013	0.003								
4	0.681	0.009	0.134	0.	0.110	0.061	0.034	0.243	0.096	0.024	0.250	0.323	0.207	0.083	0.022	0.004						
5	1.160	0.223	0.059	0.035	0.059	0.010	0.120	0.018	0.166	0.394	0.036	0.161	0.488	0.463	0.238	0.079	0.018					
6	0.987	0.519	0.005	0.038	0.001	0.031	0.009	0.034	0.079	0.005	0.344	0.219	0.006	0.306	0.490	0.337	0.137	0.037	0.007			
7	0.079	0.180	0.006	0.025	0.005	0.013	0.004	0.021	0.000	0.043	0.011	0.024	0.057	0.007	0.017	0.065	0.063	0.032	0.010	0.002		
8	0.133	0.331	0.107	0.024	0.014	0.001	0.012	0.001	0.017	0.009	0.031	0.077	0.	0.117	0.071	0.002	0.101	0.156	0.105	0.040	0.010	
9	0.002	0.013	0.010	0.	0.006	0.001	0.003	0.001	0.003	0.001	0.004	0.000	0.004	0.001	0.002	0.004	0.000	0.001	0.005	0.004	0.002	0.001
	μ_0=0.20 μ=0.60																					
0	0.010	0.035	0.055	0.053	0.035	0.016	0.006	0.002	0.000													
1	0.046	0.072	0.028	0.	0.029	0.057	0.049	0.026	0.009	0.003	0.001											
2	0.077	0.039	0.001	0.039	0.030	0.	0.020	0.047	0.042	0.022	0.008	0.002										
3	0.168	0.009	0.047	0.042	0.002	0.059	0.041	0.	0.042	0.078	0.061	0.028	0.009	0.002								
4	0.512	0.007	0.118	0.	0.094	0.050	0.027	0.175	0.066	0.016	0.166	0.215	0.138	0.055	0.015	0.003						
5	0.868	0.185	0.055	0.033	0.055	0.009	0.108	0.015	0.129	0.282	0.025	0.111	0.338	0.320	0.165	0.054	0.012					
6	0.730	0.434	0.006	0.037	0.001	0.030	0.008	0.032	0.071	0.005	0.255	0.158	0.004	0.220	0.352	0.242	0.099	0.026	0.005			
7	0.059	0.125	0.005	0.022	0.005	0.012	0.003	0.018	0.000	0.032	0.008	0.016	0.038	0.005	0.012	0.043	0.042	0.022	0.007	0.001		
8	0.099	0.253	0.082	0.021	0.014	0.001	0.012	0.001	0.016	0.008	0.025	0.058	0.	0.081	0.048	0.002	0.069	0.107	0.072	0.028	0.007	
9	0.002	0.009	0.007	0.	0.005	0.001	0.002	0.001	0.002	0.001	0.003	0.000	0.003	0.000	0.001	0.002	0.000	0.001	0.003	0.003	0.001	
	μ_0=0.20 μ=0.80																					
0	0.008	0.027	0.043	0.041	0.026	0.012	0.004	0.001	0.000													
1	0.037	0.057	0.022	0.	0.022	0.043	0.037	0.019	0.007	0.002												
2	0.062	0.031	0.001	0.031	0.023	0.	0.015	0.036	0.031	0.016	0.006	0.001										
3	0.135	0.007	0.039	0.034	0.002	0.046	0.031	0.	0.031	0.059	0.046	0.021	0.007	0.001								
4	0.411	0.006	0.106	0.	0.083	0.043	0.022	0.136	0.050	0.012	0.125	0.161	0.104	0.041	0.011	0.002						
5	0.693	0.158	0.052	0.031	0.052	0.009	0.098	0.013	0.106	0.220	0.019	0.086	0.259	0.246	0.126	0.042	0.010					
6	0.579	0.373	0.004	0.036	0.001	0.029	0.008	0.030	0.066	0.004	0.202	0.124	0.003	0.172	0.274	0.189	0.077	0.021	0.004			
7	0.047	0.096	0.004	0.020	0.004	0.011	0.003	0.016	0.000	0.026	0.006	0.012	0.029	0.004	0.009	0.032	0.032	0.016	0.005	0.001		
8	0.079	0.204	0.066	0.019	0.014	0.001	0.011	0.001	0.016	0.008	0.022	0.046	0.	0.061	0.037	0.001	0.053	0.081	0.055	0.021	0.005	
9	0.001	0.007	0.005	0.	0.003	0.000	0.002	0.001	0.002	0.000	0.002	0.000	0.002	0.000	0.001	0.002	0.000	0.001	0.002	0.002	0.001	
	μ_0=0.20 μ=1.00																					
0	0.007	0.023	0.035	0.033	0.021	0.010	0.003	0.001	0.000													
1	0.031	0.047	0.018	0.	0.018	0.034	0.030	0.016	0.006	0.002												
2	0.052	0.026	0.001	0.025	0.019	0.	0.012	0.028	0.025	0.013	0.005	0.001										
3	0.112	0.006	0.033	0.029	0.001	0.038	0.025	0.	0.025	0.047	0.037	0.017	0.005	0.001								
4	0.343	0.006	0.096	0.	0.074	0.037	0.019	0.112	0.040	0.009	0.100	0.129	0.083	0.033	0.009	0.002						
5	0.580	0.139	0.049	0.030	0.049	0.008	0.090	0.012	0.092	0.181	0.016	0.069	0.210	0.199	0.103	0.034	0.008					
6	0.480	0.328	0.004	0.035	0.001	0.028	0.008	0.029	0.062	0.003	0.168	0.102	0.003	0.141	0.225	0.155	0.063	0.017	0.003			
7	0.039	0.078	0.003	0.018	0.004	0.010	0.003	0.014	0.000	0.021	0.005	0.010	0.023	0.003	0.007	0.026	0.025	0.013	0.004	0.001		
8	0.066	0.171	0.056	0.017	0.013	0.001	0.011	0.001	0.015	0.007	0.019	0.039	0.	0.050	0.030	0.001	0.042	0.066	0.044	0.017	0.004	
9	0.001	0.005	0.004	0.	0.003	0.000	0.002	0.001	0.001	0.000	0.002	0.000	0.002	0.000	0.001	0.001	0.000	0.001	0.002	0.002	0.001	

INTENSITIES OF THE LBH BANDS (10^{-6} ERGS/CM2 SEC STRAD)

Table 4

v''	0	1	2	3	4	5	6	7	8	9	10	11	12	13	14	15	16	17	18	19	20	21
v' / μ_0=0.40 μ=0.20																						
0	0.027	0.103	0.188	0.225	0.181	0.093	0.033	0.009	0.002													
1	0.124	0.202	0.088	0.	0.131	0.304	0.292	0.155	0.057	0.015	0.003											
2	0.206	0.102	0.003	0.123	0.113	0.	0.112	0.281	0.249	0.129	0.045	0.011										
3	0.449	0.018	0.097	0.095	0.006	0.192	0.179	0.	0.247	0.468	0.366	0.168	0.053	0.012								
4	1.365	0.011	0.168	0.	0.147	0.089	0.061	0.597	0.317	0.095	0.998	1.296	0.833	0.332	0.089	0.018						
5	2.350	0.328	0.065	0.038	0.065	0.011	0.145	0.025	0.295	0.962	0.104	0.468	1.444	1.370	0.704	0.233	0.053					
6	2.104	0.710	0.005	0.040	0.001	0.033	0.009	0.038	0.096	0.008	0.701	0.466	0.013	0.780	1.247	0.859	0.350	0.094	0.017			
7	0.158	0.527	0.012	0.031	0.006	0.015	0.005	0.027	0.001	0.087	0.032	0.088	0.227	0.029	0.070	0.259	0.254	0.130	0.042	0.009		
8	0.270	0.624	0.196	0.030	0.015	0.001	0.013	0.001	0.019	0.011	0.044	0.151	0.	0.379	0.248	0.009	0.355	0.550	0.370	0.142	0.035	
9	0.005	0.052	0.040	0.	0.017	0.002	0.007	0.003	0.008	0.003	0.013	0.000	0.016	0.003	0.007	0.014	0.001	0.006	0.018	0.017	0.008	0.002
μ_0=0.40 μ=0.40																						
0	0.021	0.074	0.126	0.137	0.098	0.048	0.017	0.005	0.001													
1	0.093	0.148	0.062	0.	0.077	0.163	0.147	0.077	0.028	0.008	0.002											
2	0.155	0.077	0.003	0.086	0.073	0.	0.059	0.141	0.125	0.065	0.023	0.006										
3	0.337	0.015	0.080	0.076	0.004	0.132	0.107	0.	0.125	0.235	0.183	0.084	0.026	0.006								
4	1.027	0.010	0.156	0.	0.132	0.077	0.049	0.404	0.180	0.047	0.501	0.648	0.416	0.166	0.045	0.009						
5	1.762	0.284	0.063	0.037	0.063	0.011	0.136	0.022	0.233	0.659	0.064	0.286	0.878	0.832	0.428	0.142	0.032					
6	1.494	0.629	0.005	0.039	0.001	0.032	0.009	0.037	0.090	0.007	0.493	0.311	0.008	0.514	0.822	0.566	0.231	0.062	0.011			
7	0.118	0.321	0.009	0.029	0.006	0.014	0.004	0.024	0.001	0.065	0.020	0.047	0.114	0.015	0.035	0.130	0.127	0.065	0.021	0.004		
8	0.200	0.480	0.153	0.027	0.015	0.001	0.013	0.001	0.018	0.010	0.038	0.114	0.	0.209	0.135	0.005	0.193	0.299	0.201	0.077	0.019	
9	0.004	0.026	0.020	0.	0.011	0.001	0.005	0.002	0.005	0.002	0.007	0.000	0.008	0.001	0.004	0.007	0.001	0.003	0.009	0.008	0.004	0.001
μ_0=0.40 μ=0.60																						
0	0.016	0.058	0.095	0.098	0.068	0.032	0.011	0.003	0.001													
1	0.074	0.117	0.048	0.	0.054	0.111	0.098	0.052	0.019	0.005	0.001											
2	0.124	0.062	0.002	0.066	0.054	0.	0.040	0.094	0.083	0.043	0.015	0.004										
3	0.270	0.012	0.068	0.063	0.003	0.101	0.076	0.	0.084	0.157	0.122	0.056	0.018	0.004								
4	0.824	0.009	0.145	0.	0.121	0.068	0.041	0.305	0.126	0.032	0.334	0.432	0.278	0.111	0.030	0.006						
5	1.404	0.251	0.061	0.036	0.061	0.010	0.128	0.020	0.195	0.495	0.046	0.206	0.633	0.600	0.309	0.102	0.023					
6	1.152	0.573	0.005	0.038	0.001	0.032	0.009	0.035	0.084	0.006	0.380	0.236	0.006	0.384	0.615	0.424	0.173	0.046	0.008			
7	0.095	0.231	0.008	0.027	0.005	0.013	0.004	0.022	0.001	0.052	0.015	0.032	0.076	0.010	0.023	0.086	0.085	0.043	0.014	0.003		
8	0.158	0.389	0.125	0.025	0.015	0.001	0.012	0.001	0.018	0.010	0.034	0.091	0.	0.144	0.093	0.003	0.133	0.205	0.138	0.053	0.013	
9	0.003	0.018	0.013	0.	0.008	0.001	0.004	0.002	0.004	0.001	0.005	0.000	0.005	0.001	0.002	0.005	0.000	0.002	0.006	0.006	0.003	0.001
μ_0=0.40 μ=0.80																						
0	0.014	0.047	0.076	0.076	0.052	0.024	0.008	0.002	0.000													
1	0.062	0.097	0.039	0.	0.042	0.084	0.074	0.039	0.014	0.004	0.001											
2	0.103	0.052	0.002	0.054	0.043	0.	0.030	0.071	0.062	0.032	0.011	0.003										
3	0.225	0.011	0.059	0.054	0.003	0.082	0.059	0.	0.063	0.117	0.092	0.042	0.013	0.003								
4	0.688	0.009	0.135	0.	0.111	0.061	0.035	0.245	0.097	0.024	0.251	0.326	0.208	0.083	0.022	0.004						
5	1.178	0.225	0.059	0.035	0.059	0.010	0.121	0.018	0.169	0.397	0.036	0.161	0.492	0.466	0.240	0.079	0.018					
6	0.937	0.517	0.005	0.038	0.001	0.031	0.009	0.034	0.080	0.005	0.310	0.191	0.005	0.309	0.494	0.340	0.139	0.037	0.007			
7	0.079	0.180	0.006	0.025	0.005	0.013	0.004	0.021	0.000	0.043	0.011	0.024	0.057	0.007	0.017	0.065	0.063	0.032	0.010	0.002		
8	0.131	0.326	0.105	0.024	0.014	0.001	0.012	0.001	0.017	0.009	0.031	0.075	0.	0.110	0.071	0.002	0.101	0.156	0.105	0.040	0.010	
9	0.002	0.013	0.010	0.	0.006	0.001	0.003	0.001	0.003	0.001	0.004	0.000	0.004	0.001	0.002	0.004	0.000	0.001	0.005	0.004	0.002	0.001
μ_0=0.40 μ=1.00																						
0	0.012	0.040	0.064	0.063	0.042	0.019	0.007	0.002	0.000													
1	0.053	0.083	0.033	0.	0.034	0.068	0.059	0.031	0.011	0.003	0.001											
2	0.089	0.045	0.001	0.045	0.036	0.	0.025	0.057	0.050	0.026	0.009	0.002										
3	0.193	0.010	0.052	0.047	0.002	0.069	0.048	0.	0.050	0.094	0.073	0.034	0.011	0.002								
4	0.590	0.008	0.127	0.	0.102	0.056	0.030	0.205	0.079	0.019	0.201	0.259	0.167	0.066	0.018	0.004						
5	1.007	0.204	0.057	0.034	0.057	0.010	0.114	0.017	0.151	0.331	0.030	0.132	0.404	0.383	0.197	0.065	0.015					
6	0.788	0.468	0.005	0.038	0.001	0.031	0.009	0.033	0.075	0.005	0.262	0.160	0.004	0.258	0.413	0.285	0.116	0.031	0.006			
7	0.068	0.148	0.006	0.023	0.005	0.012	0.004	0.019	0.000	0.037	0.009	0.019	0.046	0.006	0.014	0.052	0.051	0.026	0.008	0.002		
8	0.111	0.281	0.091	0.022	0.014	0.001	0.012	0.001	0.017	0.009	0.028	0.064	0.	0.089	0.057	0.002	0.082	0.127	0.086	0.033	0.008	
9	0.002	0.011	0.008	0.	0.005	0.001	0.003	0.001	0.002	0.001	0.003	0.000	0.003	0.001	0.001	0.003	0.000	0.001	0.004	0.003	0.002	

INTENSITIES OF THE LBH BANDS (10^{-6} ERGS/CM2 SEC STRAD)

Table 4

v''	0	1	2	3	4	5	6	7	8	9	10	11	12	13	14	15	16	17	18	19	20	21
v'	μ_0=0.60 μ = 0.20																					
0	0.031	0.118	0.224	0.287	0.250	0.136	0.050	0.014	0.003													
1	0.139	0.230	0.103	0.	0.172	0.429	0.435	0.231	0.085	0.023	0.005											
2	0.232	0.114	0.004	0.143	0.138	0.	0.161	0.418	0.374	0.194	0.068	0.017										
3	0.506	0.020	0.104	0.103	0.006	0.227	0.231	0.	0.366	0.702	0.550	0.253	0.079	0.018								
4	1.541	0.012	0.174	0.	0.153	0.094	0.067	0.714	0.426	0.142	1.496	1.950	1.252	0.500	0.135	0.027						
5	2.682	0.347	0.066	0.039	0.066	0.011	0.149	0.026	0.325	1.158	0.129	0.582	1.854	1.758	0.904	0.299	0.068					
6	2.412	0.749	0.005	0.040	0.001	0.033	0.009	0.038	0.099	0.008	0.778	0.495	0.013	0.959	1.533	1.057	0.430	0.115	0.021			
7	0.178	0.671	0.013	0.032	0.006	0.015	0.005	0.028	0.001	0.098	0.041	0.126	0.339	0.044	0.104	0.389	0.381	0.195	0.062	0.013		
8	0.305	0.692	0.217	0.031	0.015	0.001	0.013	0.001	0.019	0.011	0.046	0.170	0.	0.462	0.338	0.012	0.484	0.749	0.504	0.194	0.048	
9	0.005	0.078	0.060	0.	0.022	0.002	0.008	0.004	0.009	0.003	0.017	0.000	0.024	0.004	0.011	0.022	0.002	0.009	0.027	0.025	0.012	0.003
	μ_0=0.60 μ = 0.40																					
0	0.025	0.091	0.162	0.185	0.141	0.071	0.025	0.007	0.001													
1	0.111	0.180	0.077	0.	0.106	0.236	0.220	0.116	0.043	0.011	0.002											
2	0.186	0.092	0.003	0.107	0.096	0.	0.087	0.211	0.187	0.097	0.034	0.009										
3	0.405	0.017	0.090	0.088	0.005	0.167	0.146	0.	0.187	0.352	0.275	0.126	0.040	0.009								
4	1.237	0.011	0.165	0.	0.142	0.085	0.056	0.518	0.254	0.071	0.752	0.975	0.626	0.250	0.067	0.013						
5	2.120	0.313	0.065	0.038	0.065	0.011	0.142	0.024	0.272	0.841	0.084	0.378	1.197	1.135	0.584	0.193	0.044					
6	1.803	0.682	0.005	0.040	0.001	0.033	0.009	0.038	0.094	0.007	0.562	0.346	0.009	0.666	1.065	0.734	0.299	0.080	0.015			
7	0.142	0.434	0.011	0.030	0.006	0.015	0.005	0.026	0.001	0.078	0.027	0.068	0.171	0.022	0.052	0.194	0.190	0.098	0.031	0.007		
8	0.240	0.563	0.178	0.029	0.015	0.001	0.013	0.001	0.019	0.011	0.042	0.135	0.	0.265	0.193	0.007	0.276	0.427	0.287	0.111	0.027	
9	0.004	0.039	0.030	0.	0.015	0.002	0.006	0.003	0.007	0.002	0.010	0.000	0.012	0.002	0.005	0.011	0.001	0.004	0.014	0.012	0.006	0.002
	μ_0=0.60 μ = 0.60																					
0	0.021	0.074	0.126	0.137	0.098	0.048	0.017	0.005	0.001													
1	0.093	0.148	0.062	0.	0.077	0.163	0.147	0.077	0.028	0.008	0.002											
2	0.155	0.077	0.003	0.086	0.073	0.	0.059	0.141	0.125	0.065	0.023	0.006										
3	0.338	0.015	0.080	0.076	0.004	0.133	0.107	0.	0.125	0.235	0.183	0.084	0.026	0.006								
4	1.033	0.010	0.156	0.	0.133	0.078	0.049	0.406	0.181	0.048	0.502	0.650	0.417	0.167	0.045	0.009						
5	1.777	0.286	0.063	0.038	0.063	0.011	0.136	0.022	0.234	0.655	0.063	0.280	0.882	0.836	0.430	0.142	0.033					
6	1.426	0.625	0.005	0.039	0.001	0.032	0.009	0.037	0.090	0.007	0.442	0.270	0.007	0.516	0.825	0.569	0.232	0.062	0.011			
7	0.118	0.321	0.009	0.029	0.006	0.014	0.004	0.024	0.001	0.065	0.020	0.047	0.114	0.015	0.035	0.130	0.127	0.065	0.021	0.004		
8	0.196	0.470	0.150	0.027	0.015	0.001	0.013	0.001	0.018	0.010	0.038	0.110	0.	0.187	0.135	0.005	0.193	0.299	0.201	0.077	0.019	
9	0.004	0.026	0.020	0.	0.011	0.001	0.005	0.002	0.005	0.002	0.007	0.000	0.008	0.001	0.004	0.007	0.001	0.003	0.009	0.008	0.004	0.001
	μ_0=0.60 μ = 0.80																					
0	0.018	0.062	0.104	0.108	0.075	0.036	0.013	0.003	0.001													
1	0.080	0.126	0.052	0.	0.060	0.124	0.110	0.058	0.021	0.006	0.001											
2	0.133	0.066	0.002	0.072	0.059	0.	0.045	0.106	0.094	0.049	0.017	0.004										
3	0.290	0.013	0.072	0.067	0.004	0.110	0.084	0.	0.094	0.176	0.138	0.063	0.020	0.004								
4	0.887	0.010	0.149	0.	0.125	0.072	0.043	0.334	0.141	0.036	0.377	0.488	0.313	0.125	0.034	0.007						
5	1.520	0.263	0.062	0.037	0.062	0.011	0.131	0.021	0.209	0.536	0.050	0.223	0.701	0.665	0.342	0.113	0.026					
6	1.173	0.583	0.005	0.039	0.001	0.032	0.009	0.036	0.087	0.006	0.365	0.222	0.006	0.421	0.674	0.464	0.189	0.051	0.009			
7	0.102	0.255	0.008	0.027	0.005	0.014	0.004	0.023	0.001	0.056	0.016	0.035	0.086	0.011	0.026	0.097	0.095	0.049	0.016	0.003		
8	0.165	0.402	0.129	0.026	0.015	0.001	0.012	0.001	0.018	0.010	0.035	0.093	0.	0.143	0.103	0.004	0.148	0.229	0.154	0.059	0.015	
9	0.003	0.020	0.015	0.	0.009	0.001	0.004	0.002	0.004	0.001	0.005	0.000	0.006	0.001	0.003	0.005	0.000	0.002	0.007	0.006	0.003	0.001
	μ_0=0.60 μ = 1.00																					
0	0.015	0.054	0.088	0.090	0.061	0.029	0.010	0.003	0.001													
1	0.070	0.110	0.045	0.	0.049	0.101	0.088	0.047	0.017	0.005	0.001											
2	0.116	0.058	0.002	0.062	0.050	0.	0.036	0.085	0.075	0.039	0.014	0.003										
3	0.254	0.012	0.065	0.060	0.003	0.094	0.070	0.	0.075	0.141	0.110	0.051	0.016	0.004								
4	0.777	0.009	0.142	0.	0.118	0.066	0.039	0.284	0.115	0.029	0.302	0.390	0.250	0.100	0.027	0.005						
5	1.331	0.243	0.061	0.036	0.061	0.010	0.126	0.019	0.189	0.451	0.042	0.185	0.580	0.550	0.283	0.094	0.021					
6	0.995	0.538	0.005	0.039	0.001	0.032	0.009	0.035	0.083	0.006	0.312	0.190	0.005	0.357	0.571	0.393	0.160	0.043	0.008			
7	0.089	0.211	0.007	0.026	0.005	0.013	0.004	0.022	0.001	0.049	0.013	0.029	0.069	0.009	0.021	0.078	0.076	0.039	0.012	0.003		
8	0.142	0.350	0.113	0.025	0.019	0.001	0.012	0.001	0.018	0.010	0.033	0.081	0.	0.117	0.084	0.003	0.120	0.186	0.125	0.048	0.012	
9	0.003	0.016	0.012	0.	0.007	0.001	0.004	0.001	0.003	0.001	0.004	0.000	0.005	0.001	0.002	0.004	0.000	0.002	0.005	0.005	0.002	0.001

INTENSITIES OF THE LBH BANDS (10^{-6} ERGS/CM2 SEC STRAD)

Table 4

v''	0	1	2	3	4	5	6	7	8	9	10	11	12	13	14	15	16	17	18	19	20	21
v' μ_0=0.80 μ = 0.20																						
0	0.033	0.128	0.248	0.332	0.310	0.177	0.066	0.018	0.004													
1	0.149	0.246	0.112	0.	0.204	0.539	0.577	0.308	0.113	0.030	0.006											
2	0.248	0.122	0.004	0.156	0.155	0.	0.204	0.554	0.498	0.259	0.090	0.023										
3	0.540	0.020	0.108	0.108	0.007	0.249	0.271	0.	0.483	0.935	0.734	0.337	0.106	0.024								
4	1.648	0.012	0.176	0.	0.156	0.097	0.070	0.793	0.515	0.189	1.992	2.605	1.673	0.668	0.180	0.035						
5	2.888	0.358	0.067	0.039	0.067	0.012	0.151	0.027	0.343	1.287	0.144	0.650	2.174	2.061	1.060	0.351	0.080					
6	2.608	0.771	0.005	0.040	0.001	0.033	0.010	0.039	0.100	0.008	0.816	0.493	0.013	1.087	1.739	1.198	0.488	0.131	0.024			
7	0.189	0.778	0.014	0.032	0.006	0.015	0.005	0.028	0.001	0.105	0.047	0.160	0.450	0.058	0.139	0.519	0.508	0.260	0.083	0.018		
8	0.327	0.732	0.228	0.031	0.015	0.001	0.013	0.001	0.019	0.011	0.047	0.181	0.	0.501	0.414	0.015	0.593	0.918	0.617	0.237	0.059	
9	0.006	0.103	0.079	0.	0.025	0.002	0.009	0.004	0.010	0.004	0.021	0.001	0.031	0.006	0.014	0.029	0.002	0.012	0.036	0.033	0.016	0.004
μ_0=0.80 μ = 0.40																						
0	0.027	0.103	0.188	0.225	0.181	0.093	0.033	0.009	0.002													
1	0.124	0.202	0.088	0.	0.131	0.305	0.292	0.155	0.057	0.015	0.003											
2	0.207	0.102	0.003	0.123	0.113	0.	0.113	0.281	0.250	0.130	0.045	0.011										
3	0.451	0.018	0.097	0.095	0.006	0.193	0.180	0.	0.247	0.469	0.367	0.169	0.053	0.012								
4	1.378	0.012	0.169	0.	0.148	0.090	0.061	0.603	0.319	0.095	1.003	1.303	0.837	0.334	0.090	0.018						
5	2.386	0.331	0.066	0.039	0.066	0.011	0.146	0.025	0.298	0.968	0.098	0.440	1.455	1.380	0.710	0.235	0.054					
6	2.014	0.714	0.005	0.040	0.001	0.033	0.009	0.038	0.097	0.008	0.593	0.353	0.009	0.785	1.255	0.865	0.352	0.094	0.017			
7	0.158	0.528	0.012	0.031	0.006	0.015	0.005	0.027	0.001	0.087	0.032	0.088	0.227	0.029	0.070	0.259	0.254	0.130	0.042	0.009		
8	0.266	0.615	0.194	0.030	0.015	0.001	0.013	0.001	0.019	0.011	0.044	0.148	0.	0.303	0.249	0.009	0.356	0.550	0.370	0.142	0.035	
9	0.005	0.052	0.040	0.	0.017	0.002	0.007	0.003	0.008	0.003	0.013	0.000	0.016	0.003	0.007	0.014	0.001	0.006	0.018	0.017	0.008	0.002
μ_0=0.80 μ = 0.60																						
0	0.024	0.086	0.151	0.170	0.127	0.063	0.022	0.006	0.001													
1	0.106	0.171	0.073	0.	0.097	0.212	0.196	0.103	0.038	0.010	0.002											
2	0.177	0.088	0.003	0.101	0.089	0.	0.078	0.188	0.167	0.086	0.030	0.008										
3	0.387	0.016	0.088	0.085	0.005	0.157	0.134	0.	0.166	0.313	0.245	0.112	0.035	0.008								
4	1.184	0.011	0.163	0.	0.140	0.084	0.055	0.486	0.232	0.064	0.670	0.868	0.558	0.223	0.060	0.012						
5	2.043	0.307	0.065	0.038	0.065	0.011	0.141	0.024	0.263	0.772	0.075	0.335	1.103	1.046	0.538	0.178	0.041					
6	1.617	0.662	0.005	0.040	0.001	0.033	0.009	0.037	0.094	0.007	0.471	0.281	0.008	0.622	0.994	0.685	0.279	0.075	0.014			
7	0.135	0.399	0.011	0.030	0.006	0.014	0.005	0.026	0.001	0.074	0.025	0.061	0.152	0.019	0.046	0.173	0.169	0.087	0.028	0.006		
8	0.222	0.523	0.167	0.029	0.015	0.001	0.013	0.001	0.019	0.011	0.041	0.123	0.	0.215	0.175	0.006	0.250	0.387	0.260	0.100	0.025	
9	0.004	0.035	0.027	0.	0.014	0.002	0.006	0.002	0.006	0.002	0.009	0.000	0.011	0.002	0.005	0.010	0.001	0.004	0.012	0.011	0.005	0.001
μ_0=0.80 μ = 0.80																						
0	0.021	0.074	0.126	0.137	0.098	0.048	0.017	0.005	0.001													
1	0.093	0.148	0.062	0.	0.077	0.163	0.147	0.078	0.028	0.008	0.002											
2	0.155	0.077	0.003	0.086	0.073	0.	0.059	0.142	0.125	0.065	0.023	0.006										
3	0.339	0.015	0.080	0.076	0.004	0.133	0.107	0.	0.125	0.235	0.184	0.084	0.026	0.006								
4	1.037	0.010	0.157	0.	0.134	0.078	0.049	0.407	0.182	0.048	0.503	0.651	0.418	0.167	0.045	0.009						
5	1.781	0.287	0.063	0.038	0.064	0.011	0.137	0.022	0.236	0.641	0.060	0.269	0.885	0.839	0.431	0.143	0.033					
6	1.341	0.612	0.005	0.039	0.001	0.032	0.009	0.037	0.091	0.006	0.393	0.234	0.006	0.517	0.827	0.570	0.232	0.062	0.011			
7	0.119	0.321	0.009	0.029	0.006	0.014	0.004	0.024	0.001	0.065	0.020	0.047	0.114	0.015	0.035	0.130	0.127	0.065	0.021	0.004		
8	0.188	0.452	0.145	0.028	0.015	0.001	0.013	0.001	0.019	0.010	0.038	0.105	0.	0.167	0.135	0.005	0.194	0.300	0.201	0.077		
9	0.004	0.026	0.020	0.	0.011	0.001	0.005	0.002	0.005	0.002	0.007	0.000	0.008	0.001	0.004	0.007	0.001	0.003	0.009	0.008	0.004	0.001
μ_0=0.80 μ = 1.00																						
0	0.018	0.065	0.108	0.114	0.080	0.038	0.013	0.004	0.001													
1	0.083	0.131	0.054	0.	0.063	0.132	0.118	0.062	0.023	0.006	0.001											
2	0.138	0.069	0.002	0.075	0.062	0.	0.048	0.113	0.100	0.052	0.018	0.005										
3	0.301	0.014	0.074	0.069	0.004	0.115	0.089	0.	0.100	0.188	0.147	0.067	0.021	0.005								
4	0.923	0.010	0.151	0.	0.127	0.073	0.045	0.351	0.149	0.038	0.403	0.521	0.335	0.134	0.036	0.007						
5	1.578	0.269	0.062	0.037	0.063	0.011	0.133	0.021	0.218	0.548	0.051	0.226	0.742	0.703	0.362	0.120	0.027					
6	1.140	0.577	0.005	0.039	0.001	0.032	0.009	0.036	0.088	0.006	0.338	0.202	0.005	0.442	0.707	0.488	0.199	0.053	0.010			
7	0.105	0.269	0.008	0.028	0.005	0.014	0.004	0.023	0.001	0.058	0.017	0.038	0.092	0.012	0.028	0.104	0.102	0.052	0.017	0.004		
8	0.163	0.396	0.128	0.026	0.015	0.001	0.012	0.001	0.018	0.010	0.036	0.092	0.	0.135	0.109	0.004	0.157	0.242	0.163	0.063	0.016	
9	0.003	0.021	0.016	0.	0.009	0.001	0.005	0.002	0.004	0.001	0.006	0.000	0.006	0.001	0.003	0.006	0.000	0.002	0.007	0.007	0.003	0.001

INTENSITIES OF THE LBH BANDS (10^{-6} ERGS/CM2 SEC STRAD)

Table 4

v''	0	1	2	3	4	5	6	7	8	9	10	11	12	13	14	15	16	17	18	19	20	21
v' μ_0= 1.00 μ = 0.20																						
0	0.034	0.135	0.265	0.368	0.362	0.216	0.083	0.023	0.005													
1	0.155	0.258	0.118	0.	0.230	0.637	0.716	0.384	0.142	0.038	0.008											
2	0.258	0.127	0.004	0.165	0.168	0.	0.244	0.688	0.622	0.324	0.113	0.029										
3	0.563	0.021	0.111	0.112	0.007	0.265	0.302	0.	0.596	1.167	0.917	0.422	0.132	0.030								
4	1.720	0.012	0.178	0.	0.158	0.099	0.072	0.849	0.588	0.235	2.485	3.262	2.095	0.836	0.225	0.044						
5	3.007	0.365	0.067	0.040	0.067	0.012	0.152	0.028	0.353	1.375	0.153	0.684	2.424	2.298	1.182	0.391	0.090					
6	2.743	0.786	0.005	0.040	0.001	0.033	0.010	0.039	0.101	0.008	0.835	0.480	0.012	1.186	1.896	1.307	0.532	0.143	0.026			
7	0.197	0.859	0.015	0.032	0.006	0.015	0.005	0.029	0.001	0.109	0.051	0.191	0.559	0.073	0.174	0.649	0.635	0.325	0.104	0.022		
8	0.341	0.758	0.236	0.031	0.015	0.001	0.013	0.001	0.019	0.011	0.048	0.188	0.	0.516	0.474	0.017	0.678	1.049	0.705	0.271	0.067	
9	0.006	0.127	0.098	0.	0.027	0.003	0.010	0.004	0.011	0.004	0.024	0.001	0.039	0.007	0.018	0.036	0.003	0.015	0.045	0.041	0.020	0.006
μ_0= 1.00 μ = 0.40																						
0	0.029	0.112	0.208	0.258	0.217	0.115	0.042	0.011	0.002													
1	0.133	0.218	0.096	0.	0.153	0.369	0.364	0.193	0.071	0.019	0.004											
2	0.221	0.109	0.004	0.134	0.127	0.	0.137	0.350	0.312	0.162	0.057	0.014										
3	0.483	0.019	0.101	0.100	0.006	0.212	0.208	0.	0.307	0.586	0.459	0.211	0.066	0.015								
4	1.480	0.012	0.173	0.	0.151	0.093	0.065	0.669	0.377	0.119	1.253	1.631	1.047	0.418	0.113	0.022						
5	2.575	0.342	0.066	0.039	0.066	0.011	0.148	0.026	0.315	1.065	0.107	0.478	1.679	1.593	0.819	0.271	0.062					
6	2.160	0.736	0.005	0.040	0.001	0.033	0.009	0.038	0.098	0.008	0.607	0.348	0.009	0.882	1.410	0.972	0.396	0.106	0.019			
7	0.169	0.606	0.013	0.031	0.006	0.015	0.005	0.027	0.001	0.093	0.037	0.108	0.284	0.037	0.087	0.324	0.318	0.163	0.052	0.011		
8	0.285	0.650	0.205	0.030	0.015	0.001	0.013	0.001	0.019	0.011	0.045	0.157	0.	0.320	0.296	0.010	0.424	0.656	0.441	0.170	0.042	
9	0.005	0.065	0.050	0.	0.020	0.002	0.008	0.003	0.009	0.003	0.015	0.000	0.020	0.003	0.009	0.018	0.002	0.007	0.023	0.021	0.010	0.003
μ_0= 1.00 μ = 0.60																						
0	0.026	0.095	0.171	0.199	0.155	0.078	0.028	0.008	0.002													
1	0.116	0.188	0.082	0.	0.115	0.259	0.244	0.129	0.047	0.013												
2	0.194	0.096	0.003	0.113	0.102	0.	0.095	0.235	0.208	0.108		0.010										
3	0.423	0.017	0.093	0.091	0.005	0.177	0.158	0.	0.207	0.392		0.141	0.044	0.010								
4	1.297	0.011	0.167	0.	0.145	0.087	0.059	0.552	0.278	0.079		1.087	0.698	0.279	0.075	0.015						
5	2.233	0.322	0.065	0.039	0.065	0.011	0.144	0.025	0.282	0.858	0.083	0.370	1.294	1.227	0.631	0.209	0.048					
6	1.756	0.685	0.005	0.040	0.001	0.033	0.009	0.038	0.096	0.007	0.483	0.280	0.007	0.710	1.136	0.783	0.319	0.085	0.016			
7	0.148	0.468	0.011	0.030	0.006	0.015	0.005	0.026	0.001	0.082		0.075	0.190	0.024	0.058	0.216	0.212	0.108	0.035	0.007		
8	0.240	0.559	0.178	0.029	0.015	0.001	0.013	0.001	0.019	0.011	0.043	0.132	0.	0.231	0.212	0.008	0.303	0.470	0.316	0.121	0.030	
9	0.004	0.044	0.033	0.	0.016	0.002	0.007	0.003	0.007	0.002		0.000	0.013	0.002	0.006	0.012	0.001	0.005	0.015	0.014	0.007	
μ_0= 1.00 μ = 0.80																						
0	0.023	0.083	0.145	0.162	0.120	0.059	0.021	0.006	0.001													
1	0.103	0.166	0.071	0.	0.092	0.200	0.183	0.097	0.035	0.009												
2	0.172	0.086	0.003	0.098	0.085	0.	0.073	0.177	0.156	0.081		0.007										
3	0.377	0.016	0.086	0.083	0.005	0.152	0.128	0.	0.156	0.294		0.105	0.033	0.007								
4	1.155	0.011	0.162	0.	0.139	0.083	0.054	0.469	0.220	0.060		0.815	0.524	0.209	0.056	0.011						
5	1.982	0.303	0.065	0.038	0.065	0.011	0.141	0.024	0.258	0.720	0.068	0.303	1.054	0.999	0.514	0.170	0.039					
6	1.466	0.638	0.005	0.040	0.001	0.033	0.009	0.037	0.093	0.007	0.405	0.237	0.006	0.598	0.957	0.659	0.269	0.072	0.013			
7	0.132	0.381	0.010	0.030	0.006	0.014	0.005	0.025	0.001	0.072		0.058	0.143	0.018	0.044	0.162	0.159	0.081	0.026	0.006		
8	0.206	0.486	0.156	0.028	0.015	0.001	0.013	0.001	0.019	0.011	0.060	0.114	0.	0.181	0.166	0.006	0.237	0.367	0.247	0.095	0.024	
9	0.004	0.033	0.025	0.	0.013	0.002	0.006	0.002	0.006	0.002		0.000	0.010	0.002	0.004	0.009	0.001	0.004	0.011	0.010	0.005	
μ_0= 1.00 μ = 1.00																						
0	0.021	0.074	0.126	0.137	0.098	0.048	0.017	0.005	0.001													
1	0.093	0.148	0.062	0.	0.077	0.163	0.147	0.078	0.028	0.008												
2	0.155	0.077	0.003	0.086	0.073	0.	0.059	0.142	0.125	0.065		0.006										
3	0.339	0.015	0.080	0.076	0.004	0.133	0.107	0.	0.125	0.235		0.084	0.026	0.006								
4	1.041	0.010	0.157	0.	0.134	0.078	0.049	0.408	0.182	0.048		0.652	0.419	0.167	0.045	0.009						
5	1.774	0.287	0.064	0.038	0.064	0.011	0.137	0.023	0.238	0.620	0.058	0.256	0.887	0.841	0.432	0.143	0.033					
6	1.250	0.594	0.005	0.039	0.001	0.032	0.009	0.037	0.091	0.006	0.350	0.205	0.005	0.518	0.829	0.571	0.233	0.062	0.011			
7	0.119	0.321	0.009	0.029	0.006	0.014	0.004	0.024	0.001	0.065		0.047	0.114	0.015	0.035	0.130	0.127	0.065	0.021	0.004		
8	0.179	0.429	0.138	0.028	0.015	0.001	0.013	0.001	0.019	0.010	0.038	0.099	0.	0.149	0.135	0.005	0.194	0.300	0.202	0.078	0.019	
9	0.004	0.026	0.020	0.	0.011	0.001	0.005	0.002	0.005	0.002		0.000	0.008	0.001	0.004	0.007	0.001	0.003	0.009	0.008	0.004	

lower diagram of that same figure, which corresponds to a concentration of O_2 of only 1 per cent.

The Rayleigh continuum is also plotted in Figure 1. Shortward of 1759 A, it is indeed weak compared with the band intensities. But longward of 1759 A, the continuum is about 10^5 times stronger than the bands. This will naturally rule out the possibility of any band measurements in this region.

In general, the terrestrial intensities for the bands are 5 to 10 times smaller than the Martian ones. This follows because (*a*) the O_2 content of the terrestrial atmosphere is large and (*b*) the earth's scattering atmosphere (not to be confused with the whole atmosphere) is optically thinner than that for Mars. Although the density of the Martian atmosphere at the planet's surface is smaller than is the earth's, its rarefied upper atmosphere extends to a greater height. Because of this, there are more N_2 molecules participating in the scattering in the Martian atmosphere than in that of the earth.

I am very much indebted to Dr. J. W. Chamberlain for suggesting this problem and for his continued encouragement and guidance during the course of research.

REFERENCES

Chamberlain, J W. 1961, *Physics of the Aurora and Airglow* (New York: Academic Press).
Chamberlain, J W , and Sobouti, Y. 1962, *Ap J* , **135**, 925 (Paper I).
Chandrasekhar, S. 1950, *Radiative Transfer* (Oxford: Clarendon Press).
Friedman, H 1961, *Space Research II*, eds , H. C van de Hulst, C de Jager, and A. F Moore (Amsterdam: North-Holland Publishing Co , p 1021.
Hinteregger, H. E 1961, *J. Geophys. Res* , **66**, 2367
Sobouti, Y 1962, *Ap J* , **135**, 938 (Paper II)
——— 1963*a*, *Ap J Suppl.*, **7**, 411 (No. 72)
——— 1963*b*, *Ap J* , **138**, 720 (Paper III).